

A precise determination of top quark electro-weak couplings at the ILC operating at $\sqrt{s} = 500 \text{ GeV}$

Roman Pöschl^{*†}

CNRS/IN2P3/LAL

E-mail: poeschl@lal.in2p3.fr

Top quark production in the process $e^+e^- \rightarrow t\bar{t}$ at a future linear electron positron collider with polarised beams as the International Linear Collider ILC is a powerful tool to determine indirectly the scale of new physics. The presented study, based on a detailed simulation of the ILD detector concept, assumes a centre-of-mass energy of $\sqrt{s} = 500 \text{ GeV}$ and a luminosity of $\mathcal{L} = 500 \text{ fb}^{-1}$ equally shared between the incoming beam polarisations of $\mathcal{P}, \mathcal{P}' = \pm 0.8, \mp 0.3$, respectively for the electron and positron beams. Events are selected in which the top pair decays semi-leptonically. The study comprises the cross sections, the forward-backward asymmetry and the slope of the helicity angle asymmetry. The vector, axial vector and tensorial CP conserving couplings are separately determined for the photon and the Z^0 component. The sensitivity to new physics would be dramatically improved with respect to what is expected from LHC for electroweak couplings. Details to the summary in these proceedings can be found in [1].

The European Physical Society Conference on High Energy Physics -EPS-HEP2013

18-24 July 2013

Stockholm, Sweden

^{*}Speaker.

[†]On behalf of the groups at IFIC and LAL and the ILD concept.

1. Introduction

At the International Linear Collider, ILC [2], that will collide electron and positrons at a centre-of-mass energy of 500 GeV, t quark electro-weak couplings can be measured at the % level.

In contrast to the situation at hadron colliders, the leading-order pair production process $e^+e^- \rightarrow t\bar{t}$ goes directly through the $t\bar{t}Z^0$ and $t\bar{t}\gamma$ vertices. There is no concurrent QCD production of t quark pairs, which increases greatly the potential for a clean measurement. The parametrisation of the $t\bar{t}X$ vertex can be written as:

$$\Gamma_{\mu}^{t\bar{t}X}(k^2, q, \bar{q}) = ie \left\{ \gamma_{\mu} \left(\tilde{F}_{1V}^X(k^2) + \gamma_5 \tilde{F}_{1A}^X(k^2) \right) + \frac{(q - \bar{q})_{\mu}}{2m_t} \left(\tilde{F}_{2V}^X(k^2) + \gamma_5 \tilde{F}_{2A}^X(k^2) \right) \right\}. \quad (1.1)$$

with k^2 being the four momentum of the exchanged boson and q and \bar{q} the four vectors of the t and \bar{t} quark. Further γ_{μ} are the Dirac matrices describing vector currents and γ_5 is the Dirac matrix allowing to introduce an axial vector current into the theory. The Gordon decomposition of the current defined by Eq. 1.1 leads to a useful redefinition of the form factors into:

$$\tilde{F}_{1V}^X = - (F_{1V}^X + F_{2V}^X), \quad \tilde{F}_{2V}^X = F_{2V}^X, \quad \tilde{F}_{1A}^X = -F_{1A}^X, \quad \tilde{F}_{2A}^X = -iF_{2A}^X. \quad (1.2)$$

Within the Standard Model the F_i have the following values:

$$F_{1V}^{\gamma,SM} = -\frac{2}{3}, F_{1A}^{\gamma,SM} = 0, F_{1V}^{Z,SM} = -\frac{1}{4s_w c_w} \left(1 - \frac{8}{3}s_w^2 \right), F_{1A}^{Z,SM} = \frac{1}{4s_w c_w}, \quad (1.3)$$

with s_w and c_w being the sine and the cosine of the Weinberg angle θ_w . All couplings but $F_{2A}^X(k^2)$ conserve CP .

The availability of polarised beams at the ILC allows for six independent observables. These are a) The cross section; b) The forward backward asymmetry A_{FB}^t ; c) The slope of the distribution of the helicity angle λ_t ; for two beam polarisations each. At a centre-of-mass energy of $\sqrt{s} = 500$ GeV the envisaged degree of polarisation at the ILC is 80% in case of electrons and 30% in case of positrons. With the introduced observables the six CP conserving form factors defined for the Z^0 and the photon, can be extracted simultaneously. However, the following observations apply: Close to the $t\bar{t}$ threshold the observables depend always on the sum $F_{1V} + F_{2V}$. Therefore a full disentangling of the form factors will be imprecise for energies below about 1 TeV. Hence, in the present study either the four form factors $F_{1V,A}$ are varied simultaneously, while the two F_{2V} are kept at their Standard Model values or vice versa. The CP violating form factors F_{2A}^X will be kept at their Standard Model values.

2. Experimental environment

The study has been carried out on a fully polarised sample albeit realistic values are $\mathcal{P}, \mathcal{P}' = \pm 0.8, \mp 0.3$. The cross section and therefore its uncertainty scales with the polarisation in a well defined way and the observables A_{FB}^t and λ_t vary only very mildly with the beam polarisation. Both will be correctly taken into account in the uncertainty of the results.

Signal and background events corresponding to a luminosity of 250fb^{-1} for each of the two polarisation configurations are generated with version 1.95 of the WHIZARD event generator and were subject to a full simulation of the ILD detector [2] and subsequent event reconstruction.

The decay of the top quarks proceeds predominantly through $t \rightarrow W^\pm b$. The subsequent decays of the W^\pm bosons to a charged lepton and a neutrino or a quark-anti-quark pair lead to a six-fermion final state. The study presented in this article focuses on the semi-leptonic final state $l^\pm \nu b \bar{b}' q' \bar{q}$. Several other Standard Model processes give rise to the same final state. The most important source is single-top production. Another relevant source is the WZZ production. Experimentally, ZWW production can be distinguished rather efficiently from top quark pair production. The separation between single-top production and top quark pair production is much more involved.

The entire selection procedure including lepton and b jet identification, top quark reconstruction and suppression multi-peripheral $\gamma\gamma \rightarrow \text{hadrons}$ background is explained in detail in [1]. The total selection efficiency of about 56% for semi-leptonic $t\bar{t}$ events including events with a τ lepton in the final state. Background processes can be very efficiently removed. A powerful tool is the b likeness or b -tag value that suppresses about 97% of the dominant WW background. Additional cuts comprise cuts on the t quark and W mass and of the invariant mass of the hadronic total hadronic final state.

3. Extraction of observables

With the determined efficiencies a statistical uncertainty of the $e^+e^- \rightarrow t\bar{t}$ of 0.47% in case of an initial left handed electron beam and 0.63% in case of a right handed electron beam can be estimated.

Forward-Backward Asymmetry A_{FB}^t : The forward-backward asymmetry A_{FB}^t has the well known definition

$$A_{FB}^t = \frac{N(\cos\theta > 0) - N(\cos\theta < 0)}{N(\cos\theta > 0) + N(\cos\theta < 0)}, \quad (3.1)$$

where N is the number of events in the two detector hemispheres w.r.t. the polar angle θ of the t quark calculated from the decay products in the hadronic decay branch. The direction measurement depends on the correct association of the b quarks to the jets of the hadronic b quark decays. The analysis is carried out separately for a left-handed polarised electron beam and for a right handed polarised beam. In case of a right-handed electron beam the direction of the t quark can be precisely reconstructed. In case of a left-handed electron beam the final state features two hard jets from the b quarks and soft jets from the hadronically decaying W boson. This constellation leads to migrations in the polar angle distribution of the t quark as illustrated in the left part of Fig 1 This implication motivates to restrict the determination of A_{FB}^t in case of $\mathcal{P}, \mathcal{P}' = -1, +1$ to cleanly reconstructed events. For this a test variable χ^2 is defined. The reconstructed polar angle distribution of the t quark is compared with the generated one for different cuts on χ^2 . For a value of $\chi^2 < 15$ an excellent agreement between the generated and reconstructed polar angle distributions is obtained, see the right part of Fig. 1. With this the forward backward asymmetry can be determined to a precision of about 2%.

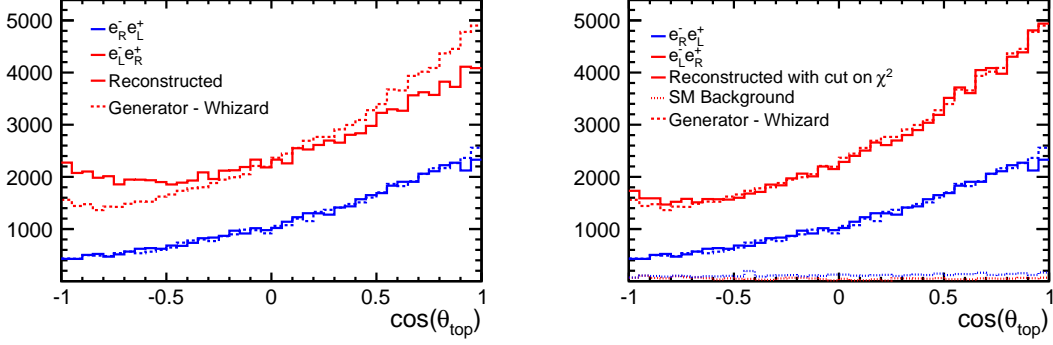


Figure 1: *Left:* Reconstructed forward-backward asymmetry compared with the prediction by the event generator WHIZARD [6] for two configurations of the beam polarisations. *Right:* The same but after the application of a cut on $\chi^2 < 15$ for the beam polarisations $\mathcal{P}, \mathcal{P}' = -1, +1$ as explained in the text. Note, that in both figures no correction is applied for the beam polarisations $\mathcal{P}, \mathcal{P}' = +1, -1$. The figure on the right hand side shows also the residual Standard Model background.

Slope of the distribution of the helicity angle λ_t : The helicity approach has been suggested for top studies at Tevatron [7]. In the rest system of the t quark, the angle of the decay leptons from the W boson θ_{hel} is distributed as:

$$\frac{1}{\Gamma} \frac{d\Gamma}{d\cos\theta_{hel}} = \frac{1 + \lambda_t \cos\theta_{hel}}{2} \quad (3.2)$$

Where λ_t varies between $+1$ and -1 depending on the fraction of right-handed (t_R) and left-handed top quarks (t_L) in the sample.

In case of μ and e , the measurement of the decay lepton is particularly simple. The Fig. 2 shows the helicity angle distribution for two configurations of the initial beam polarisation. In both cases the reconstructed distribution reproduces very well the generated one over a broad range in $\cos\theta_{hel}$. The dip at small values of $\cos\theta_{hel}$ can be explained by residual inefficiencies in the measurement of low momentum leptons. Please note that for the extraction of e.g. t quark to couplings to γ and Z^0 the slope of the distribution is used. For the determination of the slope the available lever arm is largely sufficient. The slope can be determined to a precision of about 4%.

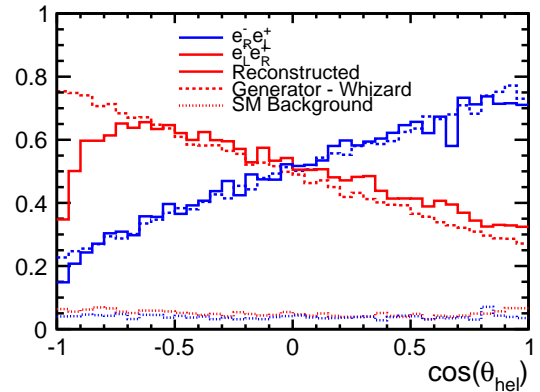


Figure 2: Polar angle of the decay lepton in the rest frame of the t quark.

4. Precision on form factors

The results on the reconstruction efficiency, A_{FB}^t and λ_t presented in the previous sections are transformed into precisions on the form factors \tilde{F}_i . The results are summarised Figure 3 and are compared with precisions obtained in a simulation study for the LHC. Note, that in the LHC study only one form factor was varied at a time while in the present study two or four form factors are varied simultaneously, see Sec. 1. From the comparison of the numbers it is justified to assume that the measurements at an electron positron collider lead to a spectacular improvement and thanks to the γ/Z^0 interference a e^+e^- collider can fix the sign the form factors. At the LHC the t quark couples either to the photon or to the Z^0 . In that case the cross section is proportional to e.g. $(F_{1V}^Z)^2 + (F_{1A}^Z)^2$. The precision expected at the LHC cannot exclude a sign flip of neither F_{1V}^Z nor of F_{1A}^Z . On the hand the LEP bounds can exclude a sign flip for F_{1A}^Z rendering a much better precision for \tilde{F}_{1A}^Z compared with \tilde{F}_{1V}^Z . Clearly, the precisions that can be obtained at the LHC are to be revisited in the light of the real LHC data. A first result on associated production of vector boson and $t\bar{t}$ pairs has been reported at this conference and is published in [8].

The expected high precision at a linear e^+e^- collider allows for a profound discussion of effects of new physics. The findings can be confronted with predictions in the framework of Randall-Sundrum models and/or compositeness models such as [9, 10, 11, 12, 13, 14] or Little Higgs models as e.g. [15]. All these models entail deviations from the Standard Model values of the t quark couplings to the Z^0 boson that will be measurable at the ILC. The interpretation of the results presented in this article in terms of the cited and maybe other models is in preparation and left for a future publication.

References

- [1] M. Amjad, M. Boronat, T. Frisson, I. Garcia, R. Poschl, *et al.*, “A precise determination of top quark electro-weak couplings at the ILC operating at $\sqrt{s} = 500$ GeV” [arXiv:1307.8102](#) [hep-ex].
- [2] T. Behnke *et al.*, “ILC TDR and DBD” *ILC-Report-2013-040*. <http://www.linearcollider.org/ILC/Publications/Technical-Design-Report>.
- [3] J.-C. Brient and H. Videau, “The Calorimetry at the future e^+e^- linear collider” *eConf C010630* (2001) E3047, [arXiv:hep-ex/0202004](#) [hep-ex].
- [4] S. Catani, Y. L. Dokshitzer, M. Seymour, and B. Webber, “Longitudinally invariant K_t clustering algorithms for hadron hadron collisions” *Nucl.Phys.* **B406** (1993) 187–224.
- [5] S. D. Ellis and D. E. Soper, “Successive combination jet algorithm for hadron collisions” *Phys.Rev.* **D48** (1993) 3160–3166, [arXiv:hep-ph/9305266](#) [hep-ph].
- [6] W. Kilian, T. Ohl, and J. Reuter, “WHIZARD: Simulating Multi-Particle Processes at LHC and ILC” *Eur.Phys.J.* **C71** (2011) 1742, [arXiv:0708.4233](#) [hep-ph].
- [7] E. L. Berger, Q.-H. Cao, C.-R. Chen, J.-H. Yu, and H. Zhang, “The Top Quark Production Asymmetries A_{FB}^t and A_{FB}^ℓ ” *Phys.Rev.Lett.* **108** (2012) 072002, [arXiv:1201.1790](#) [hep-ph].
- [8] **CMS Collaboration**, S. Chatrchyan *et al.*, “Measurement of associated production of vector bosons and top quark-antiquark pairs at $\sqrt{s} = 7$ TeV” *Phys.Rev.Lett.* **110** (2013) 172002, [arXiv:1303.3239](#) [hep-ex].

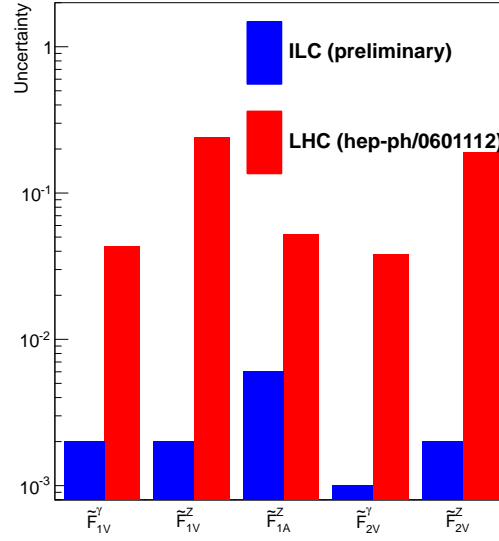


Figure 3: Comparison of statistical precisions on CP conserving form factors expected at the LHC, taken from [16] and at the ILC. The LHC results assume an integrated luminosity of $\mathcal{L} = 300 \text{ fb}^{-1}$. The results for ILC assume an integrated luminosity of $\mathcal{L} = 500 \text{ fb}^{-1}$ at $\sqrt{s} = 500 \text{ GeV}$ and a beam polarisation $\mathcal{P} = \pm 0.8$, $\mathcal{P}' = \mp 0.3$.

- [9] A. Pomarol and J. Serra, “Top Quark Compositeness: Feasibility and Implications” *Phys.Rev.* **D78** (2008) 074026, [arXiv:0806.3247 \[hep-ph\]](#).
- [10] A. Djouadi, G. Moreau, and F. Richard, “Resolving the A(FB)**b puzzle in an extra dimensional model with an extended gauge structure” *Nucl.Phys.* **B773** (2007) 43–64, [arXiv:hep-ph/0610173 \[hep-ph\]](#).
- [11] Y. Hosotani and M. Mabe, “Higgs boson mass and electroweak-gravity hierarchy from dynamical gauge-Higgs unification in the warped spacetime” *Phys.Lett.* **B615** (2005) 257–265, [arXiv:hep-ph/0503020 \[hep-ph\]](#).
- [12] Y. Cui, T. Gherghetta, and J. Stokes, “Fermion Masses in Emergent Electroweak Symmetry Breaking” *JHEP* **1012** (2010) 075, [arXiv:1006.3322 \[hep-ph\]](#).
- [13] M. S. Carena, E. Ponton, J. Santiago, and C. E. Wagner, “Light Kaluza Klein States in Randall-Sundrum Models with Custodial SU(2)” *Nucl.Phys.* **B759** (2006) 202–227, [arXiv:hep-ph/0607106 \[hep-ph\]](#).
- [14] C. Grojean, O. Matsedonskyi, and G. Panico, “Light top partners and precision physics” [arXiv:1306.4655 \[hep-ph\]](#).
- [15] C. Berger, M. Perelstein, and F. Petriello, “Top quark properties in little Higgs models” [arXiv:hep-ph/0512053 \[hep-ph\]](#).
- [16] A. Juste, Y. Kiyo, F. Petriello, T. Teubner, K. Agashe, *et al.*, “Report of the 2005 Snowmass top/QCD working group” [arXiv:hep-ph/0601112 \[hep-ph\]](#).